Nonlinear RGB-to-XYZ Mapping for Device Calibration

Weihua Xiong and Brian Funt, School of Computing Science, Simon Fraser University, Vancouver, Canada

Abstract

We introduce a new non-linear method for RGB-to-XYZ color calibration based on the technique of thin plate splines. Originally, thin plate splines were designed for deformable matching between 2-dimensional images for object recognition. We use 3-dimensional thin plate splines to map between sets of RGB device coordinates and corresponding sets of CIE XYZ coordinates. Tests calibrating several displays as well as a camera show thin plate spline calibration to be more accurate than existing linear or non-linear calibration methods.

1. Introduction

To color calibrate a display, we must generate a training set by varying its RGB input and measuring the corresponding XYZ values generated by the display. If we view the training set of RGB values as a 3D 'object' to be matched to another 3D object defined by the set of corresponding XYZ values, then we can apply thin plate splines (TPS) to calculate the mapping between them. This mapping calibrates the device since it can be used to predict the XYZ output for an RGB input not contained in the training set.

Many previous RGB-to-XYZ calibration methods have focused on linear relationships expressed in terms of a 3x3 matrix.[1-3,12] Some methods have used a look-up table with interpolation.[18] While a linear model is compact and convenient, it cannot necessarily express all the relationships in the data that a non-linear model can. The 3x3 linear models also are insufficient for devices such as digital light projector (DLP) displays that are based on 4 or more primaries.[2]

To address the limitations of linear models, others have proposed non-linear calibration methods. Vander and Haegen[15] in calibrating a camera for imaging skin lesions introduce a non-linear model involving a "de-linearizing operator" (DLO) that transforms a three-element vector into an m-element (m > 3) vector representing a higher-order polynomial transformation.

TPS has been applied successfully to many deformable registration problems.[6-9,17] Generally, it has been found to be superior to other linear and nonlinear methods in terms of stability and accuracy. It avoids a least-squares solution of an over-determined set of linear equations and it does not depend on the selection of a set of optimal parameters.

In the case of deformable 3D image registration, TPS maps each coordinate axis separately. For color calibration this means that there will be 3 separate mappings: RGB→X, RGB→Y, and RGB→Z.

Our experiments with a SONY camera and 9 display monitors show that the TPS mappings provide better calibration than the other methods tested. This result holds for the camera whether the input data are linearized to make Gamma=1 in advance or not.

2. Thin Plate Splines Introduction

A training set consists of N pairs of corresponding RGB and XYZ values $\{(R_i,G_i,B_i), (X_i,Y_i,Z_i)\}$. TPS determines parameters w_i and (a_0, a_1, a_2, a_3) controlling three non-rigid mapping functions f_X, f_Y, f_Z so

$$(X,Y,Z) = (f_X(R,G,B), f_Y(R,G,B), f_Z(R,G,B)).$$

TPS is defined by a non-linear function with an additional linear term. Without loss of generality, consider only f_X definition in which w_i and a_i are coefficients to be determined:

$$\begin{aligned} f_X(R,G,B) = &\sum_{i=1}^{N} w_i U(\|(R,G,B)-(R_i,G_i,B_i)\|) + \\ &a_0 + a_1 R + a_2 G + a_3 B \\ where \quad &U(r) = r^2 \log r \end{aligned} \tag{1}$$

Each training set pair provides defines 3 equations. For the i^{th} pair we have

$$\begin{cases} X_i = f_X(R_i,G_i,B_i) \\ Y_i = f_Y(R_i,G_i,B_i) \\ Z_i = f_Z(R_i,G_i,B_i) \end{cases} \tag{2}$$

In addition, a smoothness constraint is imposed by minimizing the bending energy. In the original TPS work,[5] the bending energy function was defined in 2D, but it generalizes to higher dimensions. For 3D RGB we have:

$$J(f_X) = \sum_{\alpha_1+\alpha_2+\alpha_3=3} \frac{3!}{\alpha_1!\alpha_2!\alpha_3!} \int \frac{\partial^3 f_X}{\partial R^{\alpha_1} \partial G^{\alpha_2} \partial B^{\alpha_3}} dRdGdB \tag{3}$$

where $J(f_X)$ is the total bending energy described in terms of the curvature of f_X. Following others,[16,21,22] the energy is minimized when

$$\begin{aligned} &\sum w_i = 0 \\ &\sum R_i w_i = 0 \\ &\sum G_i w_i = 0 \\ &\sum B_i w_i = 0 \end{aligned} \tag{4}$$

As a result, there are *(N+4)* unknowns in *(N+4)* linear equations so the TPS parameters can be found through matrix operations. Define *L* follows:

$$L = \begin{bmatrix} \bar{U} & Q \\ Q^T & O \end{bmatrix}.$$

with

$$\bar{U} = \begin{bmatrix} 0 & U_{1,2} \ldots\ldots\ldots U_{1,N} \\ U_{2,1} & 0 \ldots\ldots\ldots\ldots U_{2,N} \\ \ldots & \\ U_{N,1} \ldots\ldots\ldots\ldots\ldots\ldots 0 \end{bmatrix}$$

where $U_{ij} = U(\|(R_i,G_i,B_i) - (R_j,G_j,B_j)\|)$,

$$Q = \begin{bmatrix} 1 & R_1 & G_1 & B_1 \\ 1 & R_2 & G_2 & B_2 \\ \ldots & & & \\ 1 & R_N & G_N & B_N \end{bmatrix},$$

and *0* is the *4x4* matrix of zeroes.

Additionally define:

$W = (w_1, w_2, \ldots, w_N, a_0, a_1, a_2, a_3)^T$,

and

$K = (X_1, X_1, X_2 \ldots X_N, 0, 0, 0, 0)^T$.

We can then write $K=LW$ and solve for W as

$W = L^{-1}K$.

3. Experiments

We implemented the proposed TPS method in Matlab[19] and tested its accuracy in terms of camera calibration and display calibration. For comparison, we also implemented the non-linear de-linearization method (DLO), a linear transform applied to raw data (a special case of DLO) methods, and the standard 3x3 linear transform applied to linearized data.

3.1 Error Measures

To evaluate the effectiveness of TPS, we use three error measures. The first is the Euclidean distance between estimated XYZ values and true XYZ values; the second is the angular difference between them; and the third is ΔE2000 as defined by CIEDE2000.[13]

Given estimated $[X_e, Y_e, Z_e]$ and measured $[X_r, Y_r, Z_r]$ the distance and angular error are defined in the standard way.

$$E_{i-dist} = \sqrt{(X_e - X_r)^2 + (Y_e - Y_r)^2 + (Z_e - Z_r)^2} \quad (5)$$

The root mean square (RMS) error over a dataset of *N* samples is

$$RMS_{dist} = \sqrt{\frac{1}{N}\sum_{i=1}^{N} E_{i-dist}^2} \quad (6)$$

The angular error is

$$E_{i-angular} = COS^{-1}\left[\frac{(X_r, Y_y, Z_r)\, o\, (X_e, Y_e, Z_e)}{\sqrt{X_r^2 + Y_r^2 + Z_r^2} \times \sqrt{X_e^2 + Y_e^2 + Z_e^2}}\right] \times \frac{2\pi}{360} \quad (7)$$

3.2 Camera Calibration

The goal of calibrating color for a color camera is to find the mapping from camera RGB to the XYZ of the captured light. If the camera sensors satisfy the Luther condition[20] then in principle a calibrated camera could be used as an imaging colorimeter. We test TPS for camera calibration on the camera data from the Simon Fraser University color imaging online database.[10] The camera is a SONY DXC-930 three-chip CCD video camera and the database holds 598 RGB-XYZ pairs. Details of the data acquisition can be found in Ref. [11]. We exclude those pairs for which one or more of the RGB is 255, leaving 583 pairs.

Leave-one-out cross validation is used for testing. For each of the 583 pairs, the camera is calibrated using the other 582 pairs and then the error in predicting the remaining pair is calculated. We compute the RMS error and maximum for these 583 predictions.

Table 1 shows the results when the camera data is pre-processed to linearize the relationship between R and X, R and Y, and so forth as it is has been in the SFU dataset. Table 2 gives the corresponding results when we apply a gamma of 2 to each channel (e.g., $R^{1/2}$) to the linear data.

**Table 1: Camera calibration for linearized camera data. The table entries are the leave-one-out error as a function of method used. The methods are 3x3 linear, non-linear DLO and TPS. The errors are the maximum and root mean square of the Euclidean distance in XYZ, angular difference in XYZ, and CIEDE2000. The right hand column shows the number of predictions with $\Delta E_{2000} < 1$. **

Type	Distance		Angular		ΔE_{2000}	
	RMS	Max	RMS	Max	RMS	<1
3x3	0.03	0.22	6.10	26.0	11.5	43
DLO (m=6)	0.02	0.09	5.35	23.7	5.39	72
DLO (m=8)	0.02	0.10	3.75	18.4	4.87	110
DLO (m=11)	0.02	0.10	3.80	20.7	5.11	76
TPS	0.02	0.10	1.90	6.70	4.27	160

Table 2: Camera calibration for non-linear camera data with Gamma=2. See Table 1 caption for more detail.

Type	Distance		Angular		ΔE_{2000}	
	RMS	Max	RMS	Max	RMS	<1
3x3	0.10	0.70	6.621	26.0	6.28	5
DLO (m=6)	0.03	0.18	7.545	24.7	7.195	26
DLO (m=8)	0.03	0.15	7.260	19.5	7.260	22
DLO (m=11)	0.02	0.12	3.121	18.1	4.468	102
TPS	0.02	0.12	1.875	6.47	4.195	181

It would be helpful to know the minimal training set size required for acceptable calibration, so we varied training size from 10 to 500 to see how the error changed. For each choice of size, we extract a random training set, test on the remaining data, and calculate the RMS ΔE_{2000} error. To evaluate the likely worst-case calibration for a given training set size, we then find the maximum of these RMS errors over 150 such tests. Figure 1 plots the maximum RMS error as a function of the training set size both with and without gamma. As the training size increases, the error continues to decrease; however, the gain in accuracy becomes very marginal after the training set reaches 50 to 100 pairs.

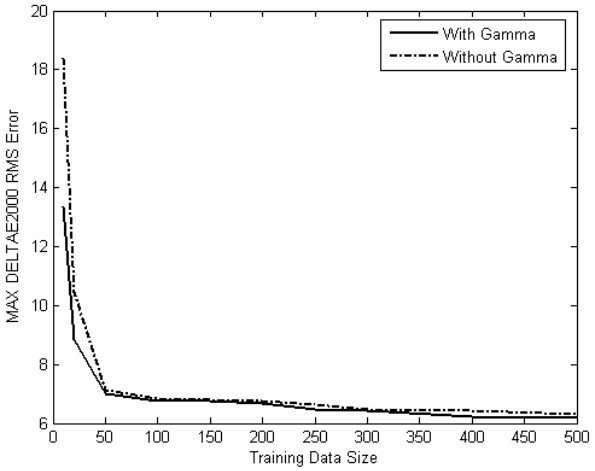

Figure 1 The Maximum ΔE_{2000} RMS Error of camera decreases as training data size increases

3.3 Display Calibration

To determine if TPS is also an effective tool for color calibration of displays, we apply it to 9 different display devices listed in Table 3. We use the calibration data for the CRTs, LCDs and projectors from Ref. [3] for which there are 1000 measured RGB-XYZ pairs sampled on a uniform 10x10x10 grid in RGB space. We use the DLP data from Ref. [4], for which there are 2273 pairs.

Table 3: Displays Used in Color Calibration Tests

Name	Display Monitor Device
CRT1	Samsung Syncmaster 900NF
CRT2	NEC Accusync 95F
LCD1	IBM 9495
LCD2	NEC 1700V
LCD3	Samsung 171N
PR1	Proxima LCD Desktop Projector 9250
PR2	Proxima LCD Ultralight LX
DLP1	Toshiba
DLP2	Infocus

We carried out a leave-one-out test similar to that for the camera calibration tests. To make the comparison across devices as comparable as possible, we selected a subset containing only 1,000 of the DLP pairs by sampling uniformly. Table 4 shows the performance comparison.

To find the minimal training dataset that can produce acceptable results, we uniformly select S values from each color channel to form the training data of size S^3. Since there are 1,000 measurements each for the CRTs, LCDs, and LCD projectors, we vary S from 3 to 8, leaving approximately half the data for testing. For DLP1 and DLP2, we vary S from 3 to 10. Figure 2 shows that as the training size is increased, the error decreases, especially until the training size reaches 216 (S=6). TPS is consistently more accurate than the other methods.

4. Conclusions

Thin plate splines are shown to be effective for color calibration of displays and a camera. Previously, these splines have been used to find deformable mappings between pairs of images. We extend them to 3-dimensions and use them to do a deformable mapping from RGB to XYZ. Although the thin-plate methods are more complex than other calibration methods, it produces more accurate results, which could be important, for example, in medical applications.

Acknowledgements

This work was supported by the Natural Sciences and Engineering Research Council of Canada.

References

1. R. S., Burns, "Methods for Characterizing CRT displays," *Displays*, Volume 16, Issue 4, pp. 173-182, 1996.
2. D., Wyble, M., Rosen, "Color Management of DLP Projectors", *Proc. IS&T/SID 12th Color Imaging Conference*, pp. 228-232, 2004.
3. B. Bastani, W. Cressman, and B. Funt, "Calibrated Colour Mapping Between LCD and CRT Displays: A Case Study," *Proc. Second European Conference on Color in Graphics, Imaging and Vision,* Achen, April 2004.
4. B. Bastani, B. V. Funt, and R. Ghaffari, "End User DLP Projector Color Calibration", *AIC'2005 Proc. 10th Congress of the International Color Association*, Granada, May 2005
5. F. L. Bookstein. "Principal warps: thin-plate splines and decomposition of deformations." *IEEE Trans. Pattern Analysis and Machine Intelligence*, 11(6):567–585, June 1989.

6. M. H. Davis, A. Khotanzad, D. Flamig, and S. Harms. “A physics-based coordinate transformation for 3-d image matching,” *IEEE Trans. Medical Imaging*, 16(3):317–328, June 1997.
7. N. Arad and D. Reisfeld, “Image warping using few anchor points and radial functions,” *Computer Graphics forum, pp.35–46*, vol. 14, pp. 35–46, 1995.
8. Asker M. Bazen and Sabih H. Gerez, “Elastic minutiae matching by means of thin-plate spline models,” *International Conference on Pattern Recognition*, Aug 2002.
9. Jitendra Malik Serge Belongie and Jan Puzicha, “Matching shapes,” *8th IEEE International Conference on Computer Vision*, Jul 2001.
10. www.cs.sfu.ca/~colour
11. K. Barnard, L. Martin, B. Funt, and A. Coath, “A Data Set for Colour Research,” *Color Research and Application,* Volume 27, Number 3, pp. 147-151, 2002.
12. M.J. Vrhel, and H.J. Trussell, “Color device calibration: A mathematical framework,” *IEEE Trans. Image Processing*, Vol. 8, pp. 1796-1806, Dec, 1999.
13. G. Sharma, W. Wu, E. N. Dalal, “The CIEDE2000 Color-Difference Formula: Implementation Notes, Supplementary Test Data, and Mathematical Observations,” *Color Research and Application*, January 2004.
14. R.L. Eubank, *Spline Smoothing and Nonparametric Regression*, Marcel Dekker, New York, 1988.
15. Y.V. Haeghen, J. Marie, A.D. Naeyaert, I. Lemahieu, and W. Philips, “An Imaging System with Calibrated Color Image Acquisition for Use in Dermatology,” *IEEE Transactions ON Medical Imaging*, Vol.19, No.7, pp. 722-730, July 2000.
16. A. Zandifar, S. Lim, R. Duraiswami, N. Gumerov, and L. S. Davis, "Multi-level Fast Multipole Method for Thin Plate Spline Evaluation,” *IEEE International Conference on Image Processing*, 2004.
17. S. Belongie, J. Malik, J. Puzicha, “Shaping Matching ND Object Recognition Using Shape Contexts,” *IEEE Transactions on PAMI*, Vol.24, No.4 pp. 509-522, 2002.
18. M.C. Stone, W.B. Cowan, and J.C. Beatty, “Color Gamut Mapping and the Printing of Digital Color Images,” *ACM Transactions on Graphics*, Vol. 7, No. 4, pp. 249-292, 1988.
19. Matlab Version 7.0.0, The MathWorks, Inc., Natick, MA, USA
20. B.K.P. Horn, “Exact Reproduction of Colored Images,” *Computer Vision, Graphics and Image Processing*, Vol. 26, No. 2, pp. 135-167, 1984.
21. F.L. Bookstein, *Morphometric Tools for Landmark Data Geometry and Biology*, Chapter 2, pp. 23-41, 1991
22. J. Meinguet, “Multivariate Interpolation at Arbitrary Points Made Simple”, *Journal of Applied Mathematics and Physics*, Vol.30, pp. 292-304, 1979

Author Biography

Weihau Xiong is a Ph.D. candidate in computing science at Simon Fraser University. His research is focussed on color especially in medical applications.

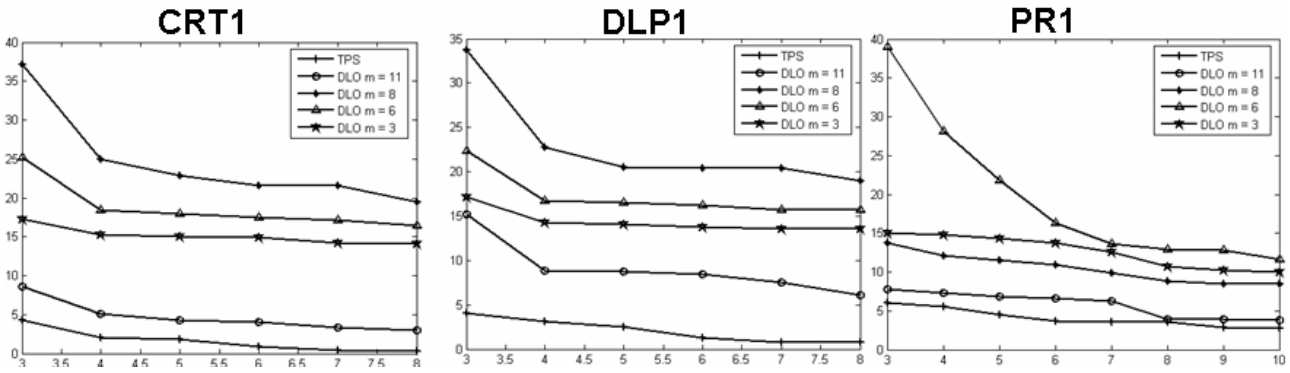

Figure 2 RMS ΔE_{2000} error for each of the three different display technologies (the other models result in similar plots) decreases as training data size increase. The horizontal axis reflects the number of samples, S, per channel so the actual training set size is S^3; the vertical axis is the corresponding RMS ΔE_{2000} RGB-to-XYZ prediction error.

Table 4: Color display calibration results in terms of RGB-to-XYZ prediction. The table entries are the leave-one-out error as a function of the method used. The methods are DLO (de-linearizing operator) linear case (M=3) applied to the raw calibration data, DLO non-linear (M>3) applied to the raw data, least-squares 3x3 linear transform after applying a separate linearization step to the data (except for the DLPs where this linearization is inappropriate), and thin plate spline interpolation (TPS) applied to the raw data. The errors are the maximum and root mean square of the Euclidean distance in XYZ, angular difference in XYZ, and ΔE2000. The right hand column shows the number of predictions with ΔE2000 < 1.

Device	Method		Distance		Angular		ΔE2000		
			RMS	Max	RMS	Max	RMS	Max	<1
CRT1	DLO Linear	M=3	0.1611	0.4463	6.4009	24.3425	13.2818	36.699	5
	DLO	M=6	0.14632	0.3567	8.6441	41.3382	15.3726	60.703	5
	DLO	M=8	0.13056	0.3689	24.6705	174.597	18.0991	65.4617	1
	DLO	M=11	0.01862	0.08502	18.6784	174.184	2.86592	21.8067	618
	LS 3x3						1.01	3.17	
	TPS		0.00584	0.02557	5.5606	174.66	0.32751	3.7678	995
CRT2	DLO Linear	M=3	0.14996	0.40065	6.40601	36.1534	11.8571	37.1721	3
	DLO	M=6	0.13637	0.34785	8.92223	54.7284	14.3185	58.1724	3
	DLO	M=8	0.12666	0.28145	22.2976	174.442	16.9171	59.1689	0
	DLO	M=11	0.00761	0.02041	1.39815	25.034	1.37686	10.6406	798
	LS 3x3						0.78	3.12	
	TPS		0.00366	0.01607	2.9576	93.272	0.21907	2.1598	995
LCD1	DLO Linear	M=3	0.17082	0.47608	7.29339	53.4337	13.0037	36.2539	2
	DLO	M=6	0.14886	0.39728	10.5131	78.8017	14.8325	45.3226	3
	DLO	M=8	0.13762	0.31911	25.9624	171.042	17.5825	62.082	0
	DLO	M=11	0.06429	0.13534	12.8953	136.659	6.0407	37.0948	28
	LS 3x3						0.44	3.12	
	TPS		0.00329	0.01585	0.60912	17.177	0.24241	2.1843	996
LCD2	DLO Linear	M=3	0.19479	0.69832	8.71708	54.6947	15.8773	40.1528	0
	DLO	M=6	0.17189	0.49652	13.4849	81.701	18.6333	62.1142	0
	DLO	M=8	0.16318	0.45034	29.8758	171.78	21.0099	61.7625	1
	DLO	M=11	0.03849	0.09604	16.4164	148.461	9.73764	49.9673	5
	LS 3x3						1.35	4.29	
	TPS		0.00556	0.02097	3.9459	124.13	0.38106	3.081	990
LCD3	DLO Linear	M=3	0.19243	0.5177	9.20738	59.121	16.5253	40.604	0
	DLO	M=6	0.16433	0.42005	12.7893	84.973	19.4618	69.2608	0
	DLO	M=8	0.15198	0.36127	28.4391	173.021	21.8315	66.4283	0
	DLO	M=11	0.04281	0.11316	20.5913	172.73	5.74086	35.7249	50
	LS 3x3						1.59	5.13	
	TPS		0.00903	0.03979	4.1319	130.02	0.35836	2.1779	990
PR1	DLO Linear	M=3	0.17039	0.45999	8.5471	69.0313	15.3383	43.0481	1
	DLO	M=6	0.15412	0.37343	13.5419	107.124	19.8696	64.1434	0
	DLO	M=8	0.14597	0.30765	25.024	168.756	21.5074	61.7837	1
	DLO	M=11	0.05939	0.14387	6.05808	68.7654	5.10661	46.6635	36
	LS 3x3						0.64	3.46	
	TPS		0.00925	0.04505	0.5604	14.827	0.5089	3.6278	960
PR2	DLO Linear	M=3	0.16187	0.39777	7.96917	60.932	14.0981	36.9653	1
	DLO	M=6	0.14546	0.32443	12.1573	96.6575	18.5984	63.8277	1
	DLO	M=8	0.13718	0.28342	23.1981	170.991	20.2858	64.4572	1
	DLO	M=11	0.07252	0.15046	10.5777	117.781	6.50392	43.1625	25
	LS 3x3						0.87	2.67	
	TPS		0.00534	0.02215	0.29534	7.21	0.27936	1.9141	992
DLP1	DLO Linear	M=3	0.19812	0.44836	5.06724	21.0655	9.18578	21.4669	1
	DLO	M=6	0.09377	0.33644	14.1473	111.189	10.6143	59.4263	59
	DLO	M=8	0.079187	0.27408	9.78453	131.179	7.82091	49.3504	84
	DLO	M=11	0.068919	0.27832	3.16055	32.8669	3.66714	12.3535	201
	TPS		0.008122	0.04383	0.24352	2.4556	0.41143	1.7767	987
DLP2	DLO Linear	M=3	0.275521	0.45350	8.05293	22.3226	13.7922	26.223	1
	DLO	M=6	0.12843	0.44261	22.6295	129.373	16.005	71.7217	17
	DLO	M=8	0.111603	0.40507	18.0235	147.961	13.0062	68.8163	16
	DLO	M=11	0.100291	0.39510	11.423	102.94	7.48642	25.8808	8
	TPS		0.006972	0.04907	0.63487	15.481	0.38952	2.1652	985